

Point defect energetics in silicon using the LDA+U method

Panchapakesan Ramanarayanan, Renat F. Sabirianov*, and Kyeongjae Cho

Department of Mechanical Engineering, Stanford University, Stanford, California 94305, USA

Fax: +1-650-723-1778, email: (panchram, kjcho)@stanford.edu

*Department of Physics, University of Nebraska, Omaha, Nebraska 68182, USA

Fax: +1-800-554-3100, email: rsabirianov@mail.unomaha.edu

We present the first principles results of point defect energetics in silicon calculated using the LDA+U method: a Hubbard type on-site interaction added to the local density approximation (LDA). The on-site Coulomb and exchange parameters were tuned to match the experimental band gap in Si. The relaxed configuration was obtained using the LDA; LDA+U was used only to calculate the energies. Our values of point defect energetics are in very good agreement with both recent experimental results and quantum Monte Carlo (QMC) calculations.

Key words: Silicon, point defects, local density approximation, Hubbard, LDA+U

1. INTRODUCTION

Modeling techniques empower the investigator with the capability to explore into the details of natural phenomena with great dexterity, aptly complementing their experimental counterparts. Hierarchical multiscale modeling (HMM) is one such technique. We have recently investigated self diffusion in silicon-germanium alloys in considerable detail by developing a database of first principles energetics and using the database to perform kinetic Monte Carlo simulations: a typical HMM scheme [1]. The exponential growth in computational processing power makes such schemes more viable; the explosive growth in nanotechnology provides technologically relevant platforms that are amenable to such schemes.

Understandably, the accuracy of the results such as those presented in Ref. [1] hinges to a great extent on the correctness of the energetics database. In that study, we used the popular local density approximation (LDA) to develop the energetics database. However, the (approximately 1 eV) discrepancy [2] between the theoretical activation energy for Si self diffusion computed using the LDA (or the generalized gradient approximation (GGA)) and the experimental values was an important reason that precluded us from making direct comparisons of our results with experimental studies of self diffusion in SiGe alloys such as those in Refs. [3, 4].

Our present work is directed essentially at finding a means of developing a reliable point defect energetics database (like in Ref. [1]) using an as parameter free a technique as possible. (While considerable progress has been made on techniques like the quantum Monte Carlo (QMC) method, it is beyond the current computational capacity to use it to develop a detailed energetics database as required for our HMM scheme.) We focus on

the activation energy for self-diffusion in pure Si. For self diffusion in Si, we consider the vacancy mechanism, the interstitialcy mechanism, and the concerted exchange mechanism. These three have been shown to be the most likely diffusion mechanisms in silicon [5, 6]. For the interstitialcy mechanism, we consider the hexagonal to split (110) mechanism as this has shown to be the most likely mechanism [7].

This article is organized as follows: In Sec. 2, we provide the details of the LDA and the LDA+U calculations. In Sec. 3, we present the results of our calculations. We provide an intuitively appealing explanation for the underperformance of the LDA. We then provide a brief overview of the LDA+U technique and discuss the results obtained using this method for the different diffusion mechanisms. We summarize our article in Sec. 4.

2. METHOD

Self-consistent electronic structure calculations were performed using the plane-wave pseudopotential code VASP [8, 9, 10, 11] with the projector augmented-wave (PAW) potentials [12] at a kinetic energy cutoff of 20 Rydberg. A 64 atom supercell was used. Electronic minimization was carried out to a tolerance of 2.7×10^{-5} eV and structures were relaxed until the maximum force on any atom was less than 0.015 eV/Å. Saddle point configuration for the hexagonal to split (110) interstitialcy mechanism was determined using the nudged elastic band method [13]. Structural relaxation was performed in two stages: initially with a 2^3 Monkhorst-Pack [14] k-point sampling followed by a 6^3 Monkhorst-Pack [14] k-point sampling. Energy calculations were done using tetrahedron method with a $6 \times 6 \times 6$ division of Brillouin zone. The lattice constant of systems containing point defects (vacancy or interstitial) was determined by

fitting the total energy versus the supercell volume to Murnaghan's equation of state*.

The plane-wave pseudopotential code VASP [8, 9, 10, 11] also has the option to perform calculations by the LDA+U method. (A brief overview of the method itself will be presented in Sec. 3. Here we merely give the details of the parameters used in our calculations.) We have used the rotationally invariant LDA+U scheme according to Liechtenstein et al. [16]. The on-site interactions were added for the p -orbitals. The effective on site Coulomb interaction parameter (U) was set to 0 eV and the effective on site exchange interaction parameter (J) was set to 4 eV. (We provide justification for this choice in Sec. 3.) The LDA was used to perform structural relaxation; the LDA+U was used only to perform energetics calculation on the structure obtained using the LDA. We adopted this approach** because the LDA gives structural properties (eg. lattice constant, see Table I) that are closer to experimental values than the LDA+U.

3. RESULTS AND DISCUSSION

Table I summarizes the results of both the LDA and LDA+U calculations. It also contains experimental values and values from quantum Monte Carlo simulations where available.

There is consensus on the values obtained within the LDA by different theoretical groups [18, 19, 7]. It can be seen that the LDA gives activation energy that is systematically lower than the experimental values.

3.1 Local density approximation

One of the main reasons for the underperformance of the LDA is that it tends to overbind. Because of this, the dangling bonds that are created due to the defects, tend to bind with each other and with other orbitals. Because of this overbinding, the energy of the system with the defect is lower than it should be in reality. Thus the difference between the energy of the pure crystal and the one with the defects (which is in fact the formation or the migration energy, depending on the situation) is lower than it should be in reality. The reason for the LDA's overbinding can be traced to the spherical nature of the exchange hole. This leads to a larger negative value of the exchange energy and hence lowers the energy of the system much more than it should be in reality [20].

A related reason for the overbinding nature is the well-known underestimation of the band gap by LDA. From our LDA based calculations, we find that, for example, the Si with a vacancy has a

band gap of only 0.88 eV in contrast to experimental values of 1.12 eV. (We note that the band gap in pure Si from LDA calculations is even less: 0.56 eV (Fig. 1). The system with the impurity has a higher band gap because of the interaction of the defect with the other atoms in the lattice. This can be seen from a simple tight binding analysis. We consider the band gap of the system with the defect because that is the environment that the defect "perceives".) Because of the small band gap, the defect states that are (usually) created in the band gap tend to interact more strongly with the valence states. This therefore leads to overbinding too. The band structure and the density of states of the system with a vacancy, hexagonal interstitial and split $\langle 110 \rangle$ interstitial are shown respectively in Figs. 2, 3, and 4.

Table I: Theoretical results and experimental values for the following properties[symbol](units) of silicon: lattice constant [L_0](Å), vacancy formation volume[†] [V_V^f](Å³), vacancy formation energy [E_V^f](eV), vacancy migration energy [E_V^m](eV), interstitial formation volume^{††} [V_I^f](Å³), hexagonal interstitial formation energy [E_{HI}^f](eV), split $\langle 110 \rangle$ interstitial formation energy [E_{SI}^f](eV), interstitial migration energy [E_I^m](eV), concerted exchange migration energy [E_{CX}^m](eV). Numbers in [] indicate reference numbers. Quantum Monte Carlo results are from Ref. [17].

Prop.	LDA	Expt.	QMC	LDA+U
L_0	5.4	5.43 [21]	—	5.27
V_V^f	4.41	—	—	—
E_V^f	3.49	4.86 [22] [‡]	—	4.59
E_V^m	0.03	—	—	0.42
V_I^f	-2.77	—	—	—
E_{HI}^f	3.37	—	4.82	4.61
E_{SI}^f	3.34	4.68 [22] [‡]	4.96	4.70
E_I^m	0.18	—	—	0.44
E_{CX}^m	4.56	—	5.78	5.82

[†] V_V^f = Relaxation volume + Atomic volume

^{††} V_I^f = Relaxation volume - Atomic volume

[‡] These values are the experimental estimates of the activation energy i.e., the sum of formation and migration energies.

There are a couple of interrelated reasons for the LDA's underestimation of the band gap. The discontinuity of the one-electron potential for localized states, which is a characteristic of the exact density functional, is absent in the LDA as was shown by Perdew *et al.* [23]. Because the band

*The Murnaghan's equation of state [15] is a relation between the energy E and the volume V of the supercell and has the following form: $E = E_0 + [(V - V_0)/b] - \{[(V^{1-a} - V_0^{1-a})V_0^a]/[(1-a)b]\}$. E_0 , V_0 , a , and b are the fitting parameters.

**We would like to point out that Leung *et al.* [17] take a similar approach: they calculate their structure using LDA and use QMC to compute the energetics.

gap can be expressed as

$$E_{gap} = E[N + 1] + E[N - 1] - 2E[N] \quad (1)$$

where $E[x]$ is the energy of the system with x electrons, the absence of the discontinuity of one-electron potential in the LDA causes the LDA to give an incorrect band gap. The second reason for the underestimation of band gap within LDA is the absence of self interaction correction. The third reason has to do with the Kohn-Sham approach [24] itself. In the Kohn-Sham theory, there is no direct relationship between the orbital energies and the ionization energies (unlike that in Hartree-Fock theory) except for the highest occupied orbital.

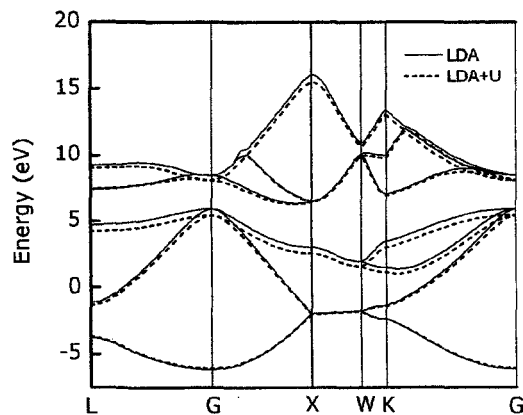


Figure 1: Si band structure computed using the LDA (solid line) and the LDA+U (dashed line) techniques. The (indirect) band gap using LDA (LDA+U) is 0.56 (0.95) eV.

3.2 Local density approximation with Hubbard type correction: LDA+U

The LDA+U method has been widely applied to metallic systems containing localized electrons. We refer the reader to the review article on LDA+U by Anisimov *et. al.* [25]. Here we provide a brief explanation of the technique along the lines of “rectifying” the deficiencies of the local density approximation that were pointed out in Sec. 3.1. The basic idea of the LDA+U method is to redistribute the electron-electron interaction. Because, as we explained in Sec. 3.1, overbinding of the localized electrons associated with the dangling bonds is a primary reason for the underperformance of the LDA, a direct way of rectifying this deficiency would be to add an on-site Coulomb repulsion term while subtracting an average overall

electron-electron interaction.

$$\begin{aligned} H_{LDA+U} &= H_{LDA} \\ &+ \sum_{i=1}^N \sum_{j=1; j \neq i}^N U_{ij} \left(\int |\psi_i(\mathbf{r}_1)|^2 d\mathbf{r}_1 \right) \\ &\times \left(\int |\psi_j(\mathbf{r}_2)|^2 d\mathbf{r}_2 \right) \\ &- U \frac{N(N-1)}{2} \end{aligned} \quad (2)$$

where $N = \sum_{i=1}^N \int |\psi_i(\mathbf{r})|^2 d\mathbf{r}$ corresponds to the total number of electrons in the system. The parameter U is adjusted by trial and error so that the resulting band gap equals the experimentally observed band gap of the system in question. The above technique, which only has the Coulomb term, is generalized to include the exchange term as well. We refer the reader to Refs. [16, 26] for more details. The $UN(N-1)/2$ term introduces the discontinuity of the one-electron potential. We wish to point out that the LDA+U does not correct for the self interaction.

As mentioned in Sec. 2, we have used the scheme as implemented in VASP for our calculations. Ideally, the Coulomb (U) and exchange (J) interaction parameters would be chosen so that the band gap for the bulk system would be equal to the experimentally observed band gap. However, because our calculations are based on a supercell geometry, there is an inevitable but unphysical interaction between the defect and the matrix. This alters the band gap from that in the bulk. However, because the system “sees” only this band gap, we have chosen U and J so that the band gap in the system with the defect is close to the experimentally observed band gap. This, of course, would mean that the parameter be tuned for each type of defect. However, for the sake of demonstration, we have worked with a single set of parameters.

We find that the defect formation and migration energies increase almost linearly with the difference: $U - J$. The best agreement between the above energies and the experimental data occurs when the calculated band gap corresponds to the experimental one. (This occurs when we choose $U = 0$ and $J = 4\text{eV}$ as mentioned in Sec. 2.) This supports our argument that the correction of the density functional for the bandgap (discontinuity of the potential on the number of electrons) should improve the results. Table I summarizes our energetics calculations. Figs. 1-4 show band structures and densities of states of the various systems considered.

3.3 Defect structure, symmetry, states and energy Vacancy:

There is an inward relaxation of the atoms around the vacancy site. The symmetry of the vacancy determines the impurity states’ symmetry. The singlet s-state is located deep inside the valence band (not shown in Fig. 2) while

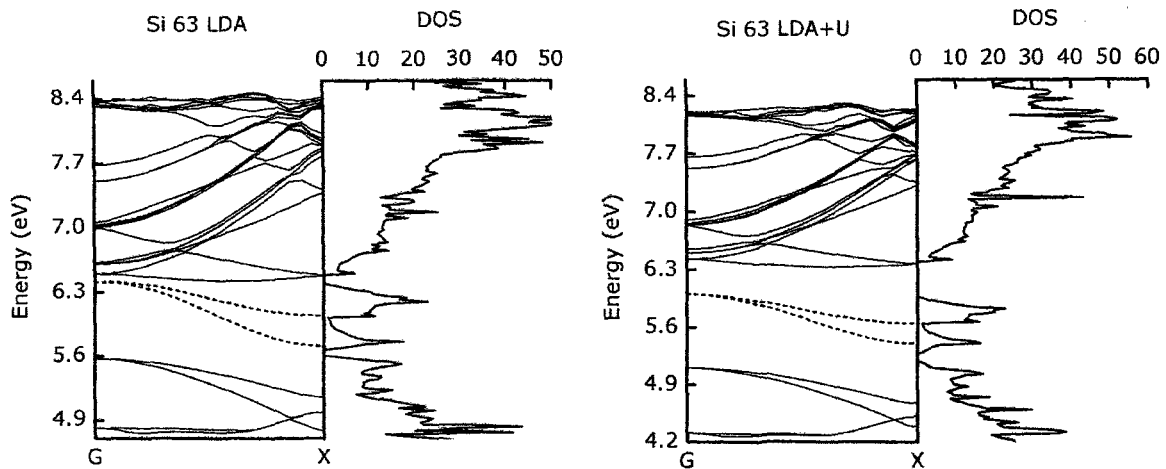


Figure 2: Band structure and density of states of a system containing a vacancy computed using the LDA (left) and the LDA+U (right) methods. The defect states are shown as dashed lines. The (indirect) band gap using the LDA (LDA+U) is 0.88 (1.21) eV and the vacancy dispersion using the LDA (LDA+U) is 0.77 (0.71) eV. The bottom vacancy state is doubly degenerate.

partly occupied triplet p-states are located in the bandgap (Fig.2). There is a splitting of p-states into twofold degenerate lower band and a single upper band (almost unoccupied). There are a few major differences between the LDA results and the LDA+U results. First, there is the expected increase in the bandgap in the LDA+U compared to the LDA leading to the separation between the vacancy states and valence and conduction bands. Second, the dispersion of vacancy p-states is smaller in the LDA+U calculation. Thus, these states are more localized in the LDA+U calculation. The dispersion cannot be removed in the supercell geometry completely, but the LDA definitely seems to overestimate the itinerancy of electrons in the vacancy states. There is no noticeable Jahn-Teller distortion of the atoms surrounding the vacancy in our 64-atom supercell geometry. This is consistent with the observation by Zywiets *et al.* [27] who suggest that a 128-atom supercell is required to observe the distortion. The formation and the migration energy for the vacancy defect from LDA+U calculations are 4.59 eV and 0.42 eV respectively. This is in good agreement with experimental results [22, 28]

Hexagonal interstitial: The self interstitial sites provide four additional electrons to the system and create similar “dangling” bonds. Like the vacancy, they create an almost doubly degenerate band near the bottom of the band gap and a single band near the top of the band gap (Fig. 3). The occupied defect states are very close to the bottom of the band gap, in agreement with the observation made by Needs [7] about the defect states being quite shallow. We find that the atoms surrounding the interstitial move outwards in contrast to the inward movement reported by Needs [7]. This is proba-

bly because, while we have optimized the lattice constant of the system with the defect, Needs has maintained the lattice constant at the experimental value. We suspect that Needs’ approach might cause an unphysical restriction on the relaxation. In addition to opening the band gap, the introduction of the on-site repulsion quite dramatically reduces the mixing of the defect states with the valence states. The formation energy for the hexagonal interstitial using the LDA+U method is 4.61 eV which is in good agreement with experimental [6] and quantum Monte Carlo [17] results.

Split $\langle 110 \rangle$ interstitial: The split $\langle 110 \rangle$ interstitial creates defect states in the band gap similar to the hexagonal interstitial except that there is a greater splitting of the two lower bands (Fig. 4). We attribute this to the lower symmetry of the split $\langle 110 \rangle$ interstitial compared to the hexagonal interstitial. Another difference is the location of the higher defect state. It is not as close to the top as in the case of hexagonal interstitial. We do not have a simple explanation for this. The introduction of the on-site repulsion has a similar effect with respect to reducing the mixing of the defect states with the bulk states. The defect formation energy using the LDA+U method is 4.70 eV which is in good agreement with the experimental [6] and quantum Monte Carlo [17] results. The migration energy from the hexagonal to the split $\langle 110 \rangle$ configurations of the interstitial was computed using the nudged elastic band method [13]. We get a value of 0.44 eV using the LDA+U method. We are not aware of any experimental result for this specific value.

3.4 Self diffusion in Si

The contribution of the mechanism to the diffu-

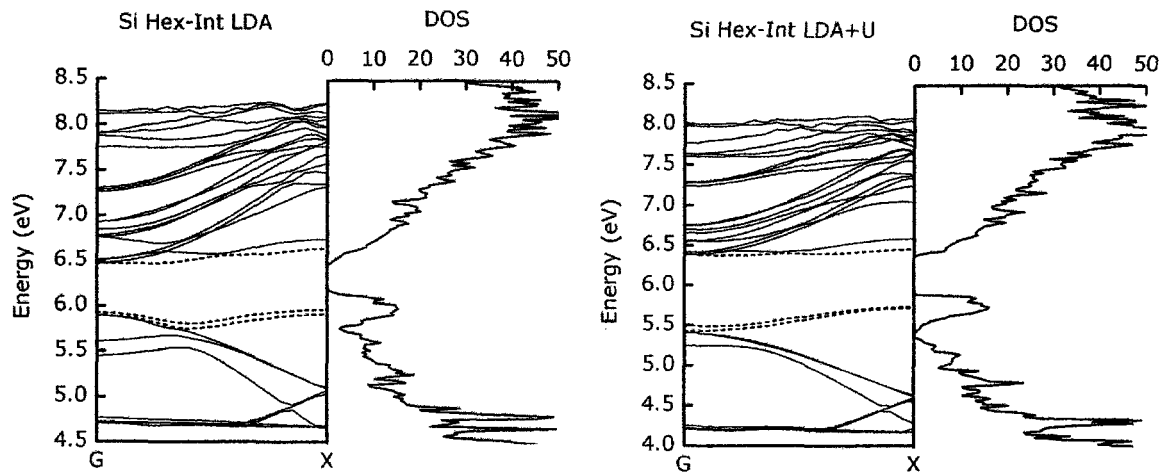


Figure 3: Band structure and density of states of a system containing a hexagonal interstitial computed using the LDA (left) and the LDA+U (right) methods. The defect states are shown as dashed lines. The (indirect) band gap using the LDA (LDA+U) is 0.70 (1.01) eV. The amount of mixing of the defect states with the valence states drops in the LDA+U method, signifying lesser binding.

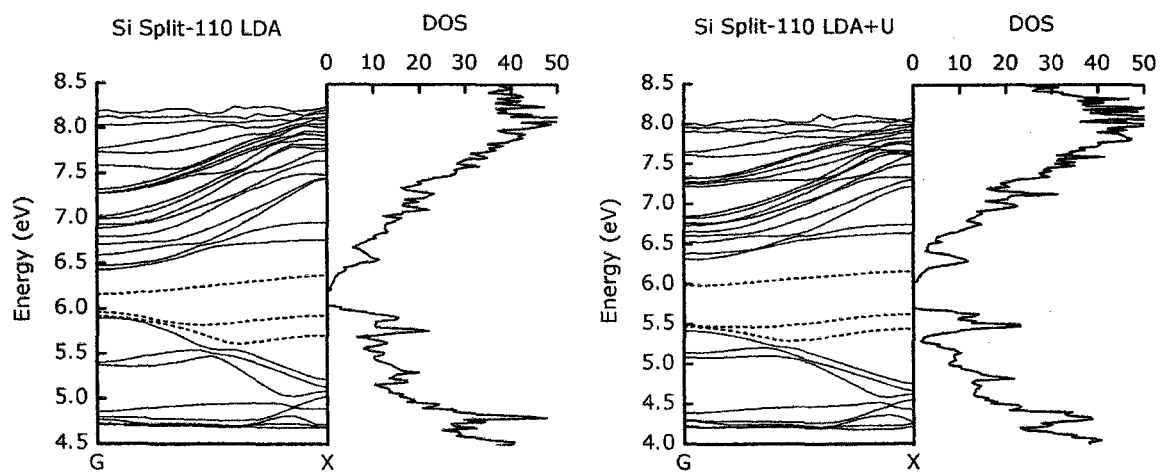


Figure 4: Band structure and density of states of a system containing a split $\langle 110 \rangle$ interstitial computed using the LDA (left) and the LDA+U (right) methods. The defect states are shown as dashed lines. The (indirect) band gap using the LDA (LDA+U) is 0.99 (1.12) eV. The amount of mixing of the defect states with the valence states drops in the LDA+U method signifying lesser binding.

sion process is determined by the activation energy and the prefactor. Because all the three mechanisms considered in this article (viz., vacancy, interstitial, and concerted exchange) involve similar number of atoms, one can, to a first approximation, assume that all of them have similar entropic effects and hence similar prefactors. Thus, based on our calculations of the activation energies using the LDA+U method, the vacancy mechanism [which has an activation energy of 5.01 eV (sum of formation (4.59 eV) and migration (0.42 eV) energies)] and the hexagonal to split (110) interstitialcy mechanism [which has an activation energy of 5.14 eV (sum of formation (4.7 eV) and migration (0.44 eV) energies)] are quite close in activation energy (within the error of the method), and should contribute equally to self-diffusion. The concerted exchange mechanism (which has an activation energy of 5.82 eV) is less significant in this respect. Experimental results give a similar indication [6, 29].

4. SUMMARY

The present work identified the cause for the poor description of point defect energetics by the LDA. It corrected for the deficiencies of the LDA by using the LDA+U method. This gave much better agreement of the calculated activation energies with experimental observations. This method can therefore be used for better description of diffusion in similar semiconductor materials.

This work was funded by the United States Department of Energy, Basic Energy Sciences Grant No. DE-FG03-99ER45788. The computations were performed on the NPACI IBM p690, NERSC IBM SP RS/6000 (as part CMSN), and on the PC clusters of the Multiscale Simulation Laboratory, Stanford: MULTIPOD and XEPOD. Grants from NPACI and NERSC are sincerely appreciated.

- [1] P. Ramanarayanan, K. Cho, and B. M. Clemens, *J. Appl. Phys.* **94**, 174–185 (2003).
- [2] M. M. D. Souza and E. M. S. Narayanan, *Defect and Diffusion Forum* **153-155**, 69–80 (1998).
- [3] N. R. Zangenberg, J. L. Hansen, J. Fage-Pedersen, and A. N. Larsen, *Phys. Rev. Lett.* **87**, 125901–1 – 125901–4 (2001).
- [4] A. Strohm, T. Voss, W. Frank, P. Laitinen, and J. Räisänen, *Z. Metallkd.* **93**, 737–744 (2002).
- [5] A. Ural, P. B. Griffin, and J. D. Plummer, *Appl. Phys. Lett.* **73**, 1706–1708 (1998).
- [6] A. Ural, P. B. Griffin, and J. D. Plummer, *J. Appl. Phys.* **85**, 6440–6446 (1999).
- [7] R. J. Needs, *J. Phys.: Condens. Matter* **11**, 10437–10450 (1999).
- [8] G. Kresse and J. Hafner, *Phys. Rev. B* **47**, 558–561 (1993).
- [9] G. Kresse and J. Hafner, *Phys. Rev. B* **49**, 14251–14269 (1994).
- [10] G. Kresse and J. Furthmüller, *Comput. Mater. Sci.* **6**, 15–50 (1996).
- [11] G. Kresse and J. Furthmüller, *Phys. Rev. B* **54**, 11169–11186 (1996).
- [12] G. Kresse and J. Joubert, *Phys. Rev. B* **59**, 1758–1775 (1999).
- [13] H. Jónsson, G. Mills, and K. W. Jacobsen, in *Classical and Quantum Dynamics in Condensed Phase Simulations*, edited by B. J. Berne, G. Ciccotti, and D. F. Coker, chapter 16, World Scientific, Singapore, 1998.
- [14] H. Monkhorst and J. Pack, *Phys. Rev. B* **13**, 5188–5192 (1976).
- [15] F. D. Murnaghan, *Proc. Natl. Acad. Sci.* **30**, 244–247 (1944).
- [16] A. I. Liechtenstein, V. I. Anisimov, and J. Zaanen, *Phys. Rev. B* **52**, R5467–R5470 (1995).
- [17] W. K. Leung, R. J. Needs, G. Rajagopal, S. Itoh, and S. Ihara, *Phys. Rev. Lett.* **83**, 2351–2354 (1999).
- [18] M. I. J. Probert and M. C. Payne, *Phys. Rev. B* **67**, 075204–1 – 075204–11 (2003).
- [19] M. J. Puska, S. Pöykkö, M. Pesola, and R. M. Nieminen, *Phys. Rev. B* **58**, 1318–1325 (1998).
- [20] W. Koch and M. C. Holthausen, *A chemist's guide to density functional theory*, Wiley-VCH, New York (2000), second edition, pp. 33–91.
- [21] C. Kittel, *Introduction to Solid State Physics*, John Wiley & Sons, Inc., New York (1996), seventh edition, pp. 23.
- [22] A. Ural, P. B. Griffin, and J. D. Plummer, *Physica B* **273-274**, 512–515 (1999).
- [23] J. P. Perdew, R. G. Parr, M. Levy, and J. Jose L. Balduz, *Phys. Rev. Lett.* **49**, 1691–1694 (1982).
- [24] W. Kohn and L. J. Sham, *Phys. Rev.* **140**, A1133–A1138 (1965).
- [25] V. I. Anisimov, F. Aryasetiawan, and A. I. Liechtenstein, *J. Phys.: Condens. Matter* **9**, 767–808 (1997).
- [26] I. V. Solovyev, P. H. Dederichs, and V. I. Anisimov, *Phys. Rev. B* **50**, 16861–16871 (1994).
- [27] A. Zywietz, J. Furthmüller, and F. Bechstedt, *Phys. Stat. Sol. (b)* **210**, 13–29 (1998).
- [28] G. D. Watkins, *Materials Science in Semiconductor Processing* **3**, 227–235 (2000).
- [29] P. Fahey, S. S. Iyer, and G. J. Scilla, *Appl. Phys. Lett.* **54**, 843–845 (1989).